NANO EXPRESS

Synthesis and Characterization of Magnetic Metal-encapsulated Multi-walled Carbon Nanobeads

A. Leela Mohana Reddy · S. Ramaprabhu

Abstract A novel, cost-effective, easy and single-step process for the synthesis of large quantities of magnetic metal-encapsulated multi-walled carbon nanobeads (MWNB) and multi-walled carbon nanotubes (MWNT) using catalytic chemical vapour deposition of methane over Mischmetal-based AB_3 alloy hydride catalyst is presented. The growth mechanism of metal-encapsulated MWNB and MWNT has been discussed based on the catalytically controlled root-growth mode. These carbon nanostructures have been characterized using scanning electron microscopy (SEM), transmission electron microscopy (TEM and HRTEM), energy dispersive analysis of X-ray (EDAX) and thermogravimetric analysis (TGA). Magnetic properties of metal-filled nanobeads have been studied using PAR vibrating sample magnetometer up to a magnetic field of 10 kOe, and the results have been compared with those of metal-filled MWNT.

Keywords Magnetic metal-filled multi-walled carbon nanobeads (MWNB) · Alloy hydride catalyst · Chemical vapour deposition · Magnetization

Introduction

Carbon nanotubes (CNTs) [1–3], including single-walled and multi-walled carbon nanotubes (SWNT and MWNT), have attracted tremendous interest both from fundamental and technological perspectives due to their unique physical and chemical properties [4]. They promise a wide range of practical applications such as catalyst supports in heterogeneous catalysis, electronic devices, field emitters, sensors, gas-storage media and molecular wires for next-generation electronic devices. Further, MWNT filled with magnetic materials have attracted a great attention due to their fundamental interest and potential applications. Electrical, thermal and mechanical properties of CNTs as well as magnetic properties of metals may be altered significantly with the introduction of ferromagnetic metals into CNTs. CNTs filled with Ni nanowires have been produced by CVD using $LaNi_2$ catalysts [5]. MWNT filled with Co and Fe have been obtained by a three-step process and their magnetic properties have been studied [6–9]. In these new types of metal-encapsulated nanostructures, the carbon shells provide an effective barrier against oxidation of metals. Therefore, these materials can be used in high-temperature magnetic applications apart from their use as electronic devices, catalysts, magnetic storage devices and sensors [10–12]. On the other hand, carbon nanotubes today represent a class of emerging materials that are capable of intracellular delivery of biologically functional peptides, proteins, nucleic acids and small molecules covalently or non-covalently attached on their surface [13–15]. The application of functionalized CNT as a new method for drug delivery was apparent immediately after the first demonstration of the capacity of this material to penetrate into cells. It is important that defects should be produced on the surface of the CNTs for the attachment of various functional materials, and therefore nanotubes are subjected to various treatments which create the defects in nanotube structure. On the other hand it may be possible to facilitate the targeted delivery of drugs in the lymphatic tissue more effectively by using a magnetic carbon nanotube [15]. Hence a defective carbon nanotube with

A. Leela Mohana Reddy · S. Ramaprabhu (✉)
Department of Physics, Alternative Energy Technology
Laboratory, Indian Institute of Technology Madras,
Chennai 600036, India
e-mail: ramp@iitm.ac.in

magnetic nature would be a proper candidate for biological applications. Metal-encapsulated carbon nanobeads, a new kind of carbon nanotubes having both defects (by its structure) and magnetic nature (due to the encapsulated metal), can be considered as one of the promising materials for drug delivery and other biological applications.

Many research groups have concentrated on the synthesis of SWNT, MWNT and metal-filled MWNT, addressing various key issues such as scale up, reproducibility and low cost. Several methods of filling of CNTs by foreign metal nanowires have been reported using capillary action, wet chemical method, arc-discharge technique, catalysed hydrocarbon pyrolysis and condensed phase electrolysis [16–19]. But many of these techniques suffer from various drawbacks such as low yield and controlled shape and size of metal-filled CNTs [20]. Hence it is important to develop a new process which will provide easy and large-scale production of CNTs and metal-filled CNTs. We have already developed a single-step technique for the synthesis of single-walled carbon nanotubes (SWNTs), multi-walled carbon nanotubes (MWNTs) and magnetic metal-filled MWNTs by fixed bed thermal chemical vapour deposition technique [21, 22]. In this paper we present a novel, cost-effective, easy and single-step process for the synthesis of metal-encapsulated multi-walled carbon nanobeads (MWNB) in large quantity which have these defects present already. Catalytic chemical vapour deposition (CCVD) technique using a single-reaction zone facility has been used to grow these nanostructures in the temperature range of 850–950 °C using Mischmetal (Bharat Rare Earths Metals, India; composition—Ce 50%, La 35%, Pr 8%, Nd 5%, Fe 0.5% and other rare earth elements 1.5%)-based AB_3 (B = Ni/Fe/Co) alloy hydride catalyst, obtained through a hydrogen-decrepitation technique. The as-grown and purified samples have been characterized using TGA, SEM, TEM, HRTEM and EDAX. Magnetic properties of metal-filled MWNB have been studied using a PAR vibrating sample magnetometer up to a magnetic field of 10 kOe, and the results have been discussed by comparing with those of metal-filled MWNT. In addition, using the catalytically controlled root-growth mode, the growth mechanism of metal-encapsulated MWNB and MWNT has been discussed.

Experimental Section

Catalyst Preparation

Mm-based AB_3 (B = Ni/Fe/Co) alloys were prepared by arc melting the constituent elements in a stoichiometric ratio under argon atmosphere. The alloy buttons were re-melted six times by turning them upside down after each solidification to ensure homogeneity. Single-phase formation of alloys was confirmed by powder X-ray diffraction. Each of these alloys was then hydrogenated to their maximum storage capacity of about 1.5 wt% using a high-pressure Seivert's apparatus. Fine powders of alloys, with fresh surfaces, were obtained with several cycles of hydrogen absorption and desorption.

Synthesis, Characterization and Magnetization Measurements of Metal-Encapsulated MWNB

The growth of carbon nanostructures has been carried out using a single-stage furnace with precisely controlled temperatures in the range 850–950 °C. Fine powders of alloy obtained after several cycles of hydrogen absorption/desorption were directly placed in a quartz boat and kept at the centre of a quartz tube, which was placed inside a tubular furnace. Hydrogen (50 sccm) was introduced into the quartz tube for 1 h at 500 °C, to remove the presence of any oxygen on the surface of the alloy hydride catalysts. Hydrogen flow was then stopped, and the furnace was heated up to the desired growth temperature followed by the introduction of methane at a flow rate of 100 sccm. Pyrolysis was carried out for 30 min and thereafter furnace was cooled to room temperature. Argon flow was maintained throughout the experiment. The carbon soot obtained in the quartz boat was purified by air oxidation and acid treatment [23] and was analysed by SEM, TEM, HRTEM, EDAX and TGA. Magnetization measurements of metal-encapsulated MWNB and MWNT were carried out using a PAR vibrating sample magnetometer at 30 °C up to a magnetic field of 10 kOe.

Results and Discussion

Mm-based AB_3 alloys, after several hydrogen absorption/desorption cycles, were found to be finely powdered to about 5–10 μm due to the plastic deformation of these alloys upon hydrogenation/dehydrogenation cycles. These hydride catalysts prepared using the hydrogen decrepitation technique provide fresh surfaces with a large surface area, free from oxidation for the growth of CNTs. High hydrogen absorption, large decrepitation and low cost make these hydrides better catalysts for large-scale production of CNTs. Experiments have been carried out using Mm-based AB_3 alloy hydride catalyst with Ni at the B site at growth temperatures of 850 and 950 °C, keeping all other parameters same. Interestingly, different types of carbon nanostructures have been observed at these two different growth temperatures. At 850 °C, Ni-encapsulated

MWNB were obtained, while at 950 °C, Ni-encapsulated MWNT could be observed. These carbon nanostructures have been characterized using SEM, TEM and HRTEM.

Figure 1a–c shows the SEM, TEM and HRTEM images of Ni-filled MWNB obtained at 850 °C. From these figures it is clear that good quality of MWNB has been obtained by CCVD technique using Mm-based AB$_3$ alloy hydride catalyst. Ni nanobeads (as confirmed from EDAX pattern, shown in Fig. 1d) of ~10-nm thickness were uniformly filled inside the full cavity of nanobead. HRTEM (Fig. 1c) shows the single crystallinity of Ni-encapsulated MWNB. Digital TEM images of the Ni-encapsulated region, such as those shown in Fig. 1c, were analysed by fast Fourier transform (FFT) techniques to reveal details of the local Ni structure. The inset to Fig. 1c is a corresponding FFT obtained for the Ni-encapsulated region of Fig. 1c. The nanorod structure can be indexed to hexagonal structure. Figure 2a–c shows the SEM, TEM and HRTEM images of Ni-filled multi-walled carbon nanotubes obtained at 950 °C. Figure 2c shows the uniform encapsulation of Ni (Fig. 2d) single crystalline MWNT. Further, the HRTEM image reveals the multi-walled nature of carbon nanotubes with each graphene layer being clearly distinguishable since the graphene sheets with a spacing of ~0.34 nm are stacked parallel to the growth axis of carbon nanotubes.

The FFT of the Ni-encapsulated region shows the hexagonal structure (Inset Fig. 2c).

A root-growth mechanism [24] could be responsible for the growth of metal-filled MWNB and MWNT. In the present study, as the size of the alloy hydride catalyst particles is seen to be in the range of 5–10 µm, we propose that each alloy hydride particle would be composed of a number of catalytic centres, which could act as nucleation sites for the growth of CNTs. There could be a further reduction in the catalyst particle size during the hydrogen treatment before the carbon deposition. Further, nickel, iron or cobalt particles are well interspersed in the alloy, allowing better dispersion of the active catalytic sites. This would further result in lesser sintering of the particles. Here, the possible growth mechanism could be through the precipitation of carbon in the form of MWNT from the molten catalytic particles. The melting temperatures of the alloy-C system are lower than those of the metal-C system. Further, the reduction in particle size lowers the melting point, which in turn affects the diffusion rate of carbon and thus changes the growth rate of CNTs [25, 26]. According to two widely accepted 'tip-growth' and 'root-growth' mechanisms, the hydrocarbon gas decomposes on the metal surfaces of the metal particle to release carbon, which dissolves in these metal particles. The dissolved carbon

Fig. 1 (**a**) SEM, (**b**) TEM, (**c**) HRTEM, FFT (Inset) and (**d**) EDAX patterns of Ni-encapsulated MWNB
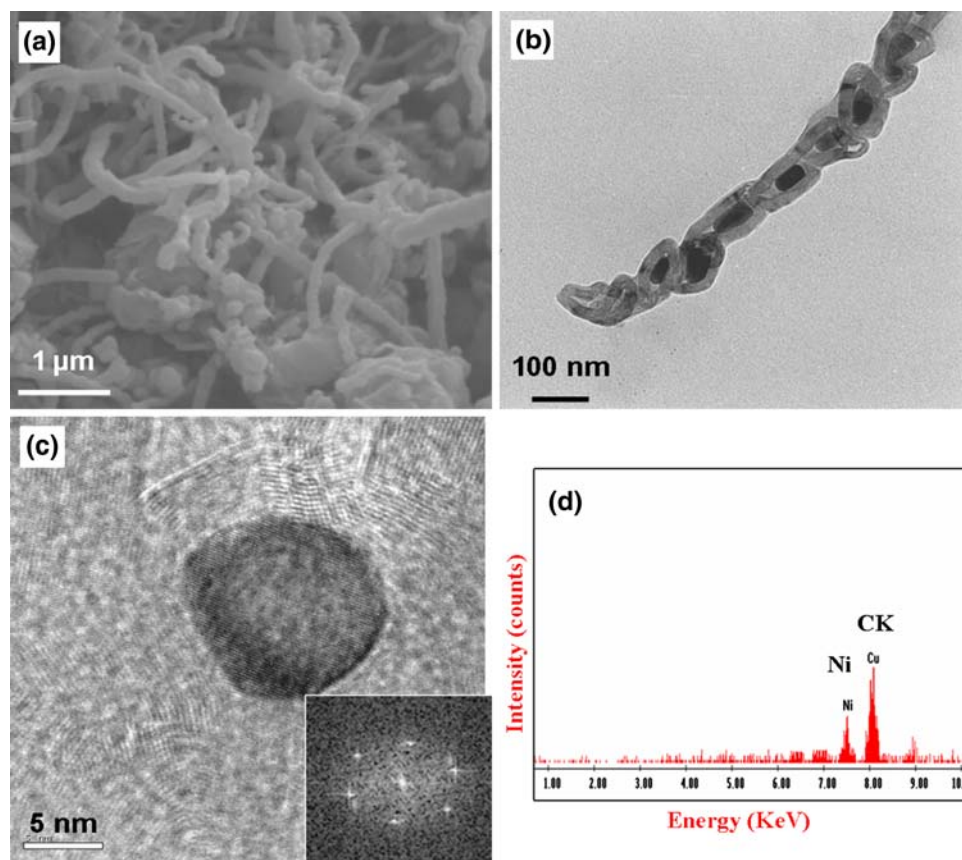
Fig. 2 (**a**) SEM, (**b**) TEM, (**c**) HRTEM, FFT (Inset) and (**d**) EDAX patterns of Ni-encapsulated MWNT
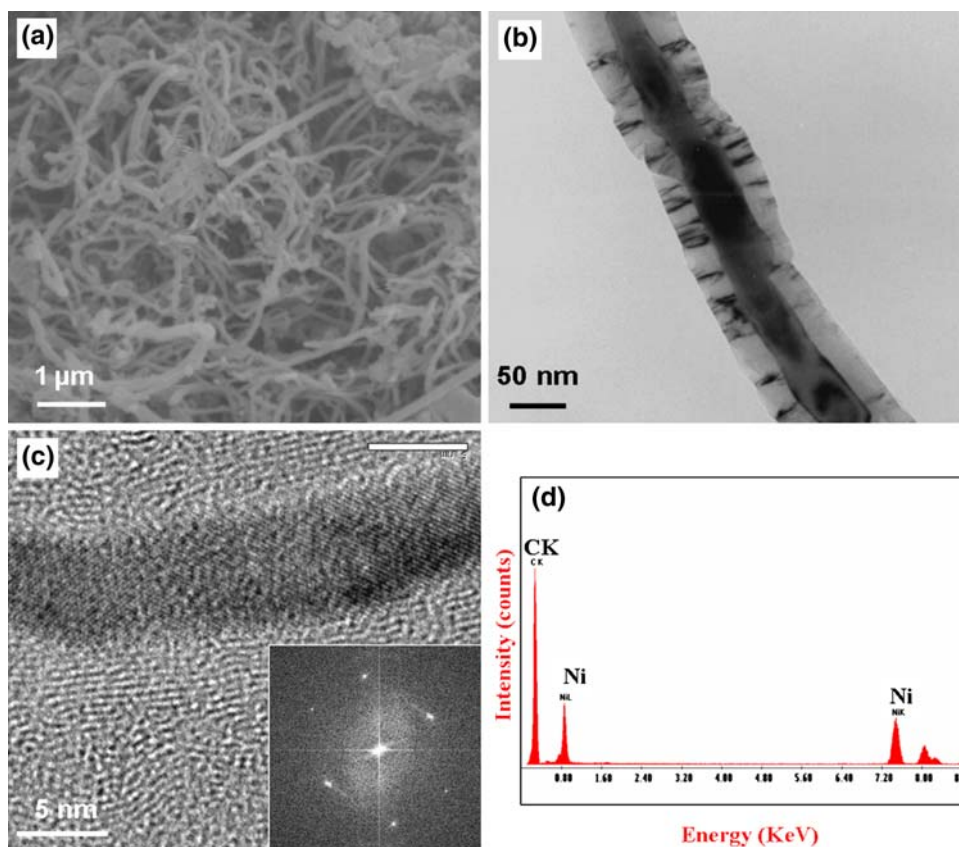

diffuses through the particle and gets precipitated to form the body of the filament. The saturated metal carbides have lower melting points. Hence they are fluid-like during the growth process resulting in their easy encapsulation due to the capillary action of the nanotube process. The encapsulated fluid results in solid metal nanowire. Thus the growth process is by the vapour–liquid–solid (VLS) mechanism, which is catalytically controlled with the capillary action of nanotubes. Figures 1 and 2 show encapsulated MWNB and MWNT, grown at 850 and 950 °C, respectively, over Mm-based AB$_3$ alloy hydride catalysts containing Ni at the B site. These structures have the uniform and complete encapsulation of Ni in the form of nanobeads and nanowires.

The temperature-programmed oxidation technique allows one to find the relative amounts of defective and crystalline constituents in the CNTs grown on different catalysts. In this process one can see that less ordered crystalline CNTs will react preferentially with the oxidant and lose weight at a lower temperature compared with more crystalline CNTs. TGA of as-grown and purified Ni-encapsulated MWNB and MWNT tell about the purity and the quantity of Ni encapsulated in the CNTs. Figure 3 shows the TGA curves of as-grown and purified Ni-encapsulated MWNB and MWNT. A slight weight gain is observed below

200 °C for the as-grown samples (Fig. 3a, b), which is due to the oxidation of catalytic metals [27], while burning of amorphous carbon results in the weight loss up to ∼500 °C, which is not seen for the purified samples. Further, weight loss between 500 and 850 °C is attributed to the burning of graphitic layers of nanotubes and a slight weight gain at 850 °C of Ni-encapsulated MWNB may be due to the formation of higher oxides of metal after complete burning of graphitic layers of MWNT. The residual weight of 40% and 43% of as-grown Ni-encapsulated MWNB and MWNT, respectively, is resulted from weight of the catalytic impurities along with encapsulated metals present in the sample. Upon purification, residual weights of 22% and 36% (Fig. 3c, d) were observed for Ni-filled MWNB and MWNT, respectively, which means that 22% and 36% of Ni are present in MWNB and MWNT, respectively.

Magnetization measurements were carried out on the metal-encapsulated MWNB and MWNT using a PAR vibrating sample magnetometer at 300 K up to a magnetic field of 10 kOe. Figure 4 shows the magnetization curves for Ni-encapsulated MWNB and MWNT synthesized using Mm-based AB$_3$ alloy hydride catalysts at temperatures of 850 and 950 °C, respectively. The saturation magnetization for Ni-encapsulated MWNB was 15 emu/g, whereas for Ni-encapsulated MWNT it was 22 emu/g due to the
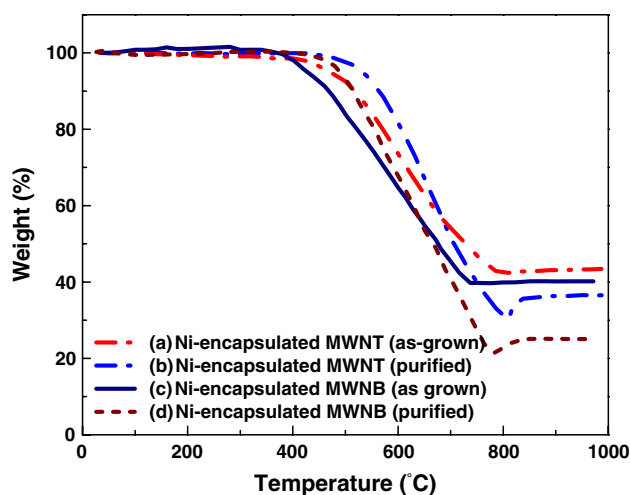
Fig. 3 TGA of as-grown and purified Ni-filled MWNB and MWNT [21]
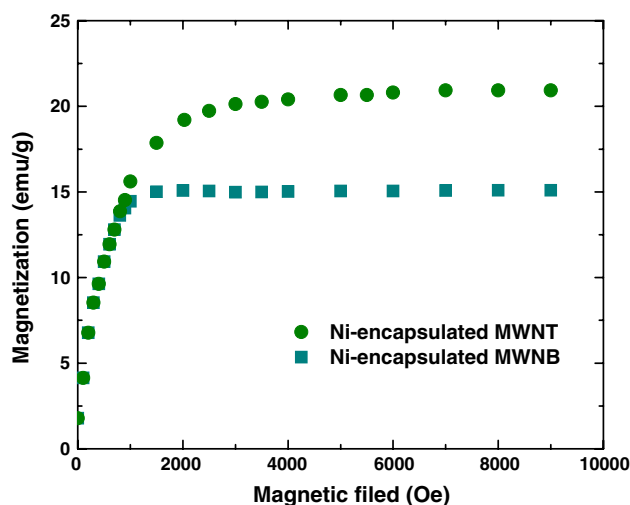
Fig. 4 Magnetization curves of Ni metal-filled MWNB and MWNT [21]

discontinuous capillary filling of Ni during the growth process. The saturation magnetization values of metal-encapsulated MWNB and MWNT obtained by the present single-step CVD method using alloy hydride catalyst are comparable with those of the carbon-coated nanoparticles [28] and metal-filled CNTs [6, 7] obtained from the three-step process. The applications of these materials for energy and biological aspects are in progress.

Conclusion

A single-step process for the synthesis of good quality and large quantities of metal-encapsulated MWNB and MWNT by a thermal CVD technique using alloy hydride catalysts

has been developed. The growth mechanism of metal-encapsulated MWNB and MWNT has been discussed based on the catalytically controlled root-growth mode. Saturation magnetization of Ni-encapsulated MWNB shows lower value compared to that of Ni-encapsulated MWNT due to the discontinuous filling of Ni during the growth process.

References

1. S. Iijima, Nature **354**, 56 (1991)
2. S. Iijima, T. Ichihashi, Nature **363**, 603 (1993)
3. D.S. Bethune, C.H. Kinang, M.S. de Vries, G. Gorman, R. Savoy, J. Vazquez, R. Bayers, Nature **363**, 605 (1993)
4. P.M. Ajayan, Chem. Rev. **99**, 1787 (1999)
5. X.P. Gao, Y. Zhang, X. Chen, G.L. Pan, J. Yan, F. Wu, H.T. Yuan, D.Y. Song, Carbon **42**, 47 (2004)
6. J. Bao, C. Tie, Z. Xu, Z. Suo, Q. Zhou, J. Hong, Adv. Mater. **14**, 1483 (2004)
7. G. Korneva, H. Ye, Y. Gogotsi, D. Halverson, G. Friedman, J.C. Bradley, K.G. Kornev, Nano Lett. **5**, 879 (2005)
8. A. Leonhardt, M. Ritschel, R. Kozhuharova, A. Graff, T. Muhl, R. Huhle, I. Monch, D. Elefant, C.M. Schneider, Diamond. Relat. Mater. **12**, 790 (2003)
9. A. Leonhardt, S. Hampel, C. Muller, I. Monch, R. Koseva, M. Ritschel, D. Elefant, K. Biedermann, B. Buchner, Chem. Vap. Deposition **12**, 380 (2006)
10. G. Che, B.B. Lakshmi, C.R. Martin, E.R. Fisher, Langmuir **15**, 750 (1999)
11. J. Sloan, J. Cook, M.L.H. Green, J.L. Hutchison, R. Tenne, J. Mater. Chem. **7**, 1089 (1997)
12. R. Kozhuharova, M. Ritschel, D. Elefant, A. Graff, I. Monch, T. Muhl, C.M. Schneider, A. Leonhardt, J. Magn. Magn. Mater. **290**, 250 (2005)
13. I. Moench, A. Meye, A. Leonhardt, in *Series: Nanotechnologies for the Life Sciences*, vol. 6, ed. by C.S.S.R. Kumar (Wiley-VCH, 2006), p. 259
14. N.W.S. Kam, H.J. Dai, J. Am. Chem. Soc. **127**, 6021 (2005)
15. A. Bianco, K. Kostarelos, M. Prato, Curr. Opin. Chem. Biol. **9**(6), 674 (2005)
16. (a) P.M Ajayan, S. Iijima, Nature **361**, 333 (1993); (b) P.M. Ajayan, T.W. Ebbesen, T. Ichihashi, S. Ijima, K. Tanigaki, H. Hiura, Nature **362**, 522 (1993)
17. (a) S.C. Tsang, Y.K. Chen, P.J.F. Harris, M.L.H. Green, Nature **372**, 159 (1994); (b) A. Chu, J. Cook, J.R. Heesom, J.L. Hutchison, M.L.H. Green, J. Sloan, Chem. Mater. **8**, 2751 (1996); (c) R.M. Lago, S.C. Tsang, K.L. Lu, Y.K. Chen, M.L.H. Green, J. Chem. Soc. Chem. Commun. 1355 (1995); (d) S.C. Tsang, J.J. Davis, M.L.H. Green, H.A.O. Hill, Y.C. Leung, P.J. Sadler, J. Chem. Soc. Chem. Commun. 1803 (1995); (e) Y.L. Hsin, K.C. Hwang, F.-R. Chen, J.-J. Kai, Adv. Mater. **13**, 830 (2001); (f) S. Fullam, D. Cottell, H. Rensmo, D. Fitzmaurice, Adv. Mater. **12**, 1430 (2000)
18. (a) S. Subramoney, Adv. Mater. **10**, 1157 (1998); (b) J.Y. Dai, J.M. Lauerhaas, A.A. Setlur, R.P.H. Chang, Chem. Phys. Lett. **258**, 547 (1996)
19. (a) N. Grobert, M. Terrones, O.J. Osborne, H. Terrones, W.K. Hsu, S. Trasobares, Y.Q. Zhu, J.P. Hare, H.W. Kroto, D.R.M. Walton, Appl. Phys. A **67**, 595 (1998); (b) A.K. Pradhan,

T. Kyotani, A. Tomita, Chem. Commun. 1317 (1999); (c) T. Kyotani, L.F. Tsai, A. Tomita, Chem. Commun. 701 (1997)

20. B.K. Pradhan, T. Toba, T. Kyotani, A. Tomita, Chem. Mater. **10**, 2510 (1998)
21. A. Leela Mohana Reddy, M.M. Shaijumon, S. Ramaprabhu, Nanotechnology **17**(21), 5299–5305 (2006)
22. M.M. Shaijumon, A. Leela Mohana Reddy, S. Ramaprabhu, Nanoscale Res. Lett. **2**(2), 75 (2007)
23. M.M. Shaijumon, S. Ramaprabhu, Chem. Phys. Lett. **374**, 513 (2003)
24. S.B. Sinnott, R. Andrews, D. Qian, A.M. Rao, Z. Mao, E.C. Dickey, F. Derbyshire, Chem. Phys. Lett. **315**, 25 (1999)
25. C. Bower, O. Zhou, W. Zhu, D.J. Werder, S. Jin, Appl. Phys. Lett. **77**, 2767 (2000)
26. C.J. Smithells, in *Smithells' Metals Reference Book*, 7th edn., ed. by E.A. Brandes, G.B. Brook (Butterworth-Heinemann Ltd., 1992)
27. M.M. Shaijumon, N. Bejoy, S. Ramaprabhu, Appl. Surf. Sci. **242**, 192 (2005)
28. R. Fernández-Pacheco, M.R. Ibarra, J.G. Valdivia, C. Marquina, D. Serrate, M.S. Romero, M. Gutiérrez, J. Arbiol, NanoBiotechnology **1**, 300 (2005)